THERMAL-HYDRAULIC MODELING OF REACTIVITY ACCIDENTS IN MTR REACTORS

by

Hany KHATER[1], Talal ABU-EL-MATY[2], and Salah EL-DIN EL-MORSHDY[2]

Received on August 30, 2006; accepted in revised form on September 26, 2006

This paper describes the development of a dynamic model for the thermal-hydraulic analysis of MTR research reactors during a reactivity insertion accident. The model is formulated for coupling reactor kinetics with feedback reactivity and reactor core thermal-hydraulics. To represent the reactor core, two types of channels are considered, average and hot channels. The developed computer program is compiled and executed on a personal computer, using the FORTRAN language. The model is validated by safety-related benchmark calculations for MTR-TYPE reactors of IAEA 10 MW generic reactor for both slow and fast reactivity insertion transients. A good agreement is shown between the present model and the benchmark calculations. Then, the model is used for simulating the uncontrolled withdrawal of a control rod of an ETRR-2 reactor in transient with over power scram trip. The model results for ETRR-2 are analyzed and discussed.

Key words: reactivity insertion accident, research reactor, thermal-hydraulic, safety analysis

INTRODUCTION

In recent years, a general interest in the evaluation of the performance and operational characteristics of research reactors has been generated by the International Atomic Energy Agency (IAEA). This interest is directed towards developing simulation programs for PC use and is concentrated on thermal-hydraulic calculations for research reactor transients. The analysis of the transient behavior of research reactors has received great attention since Woodruff [1], till Mirza *et al*., [2], Nasir *et al*., [3], and Housiadas [4], because of its inability to determine the limits of clad melting temperature. In fact, so far, research reactor safety analysis has been performed using conservative computational tools [5-9]. International thermal-hydraulic codes, currently in use for research reactors, are capable of simulating most reactor transients, but these computer codes are not accessible to a lot of researchers. Generally, the use of large codes requires a considerable amount of effort and skill regarding, in particular, input preparation and output processing. Sometimes, large codes cannot offer all the details that the reactor operators need to know about the initiating events during the proposed accident scenarios, such as reactivity insertion due to control rod withdrawal, which may be finished or fixed (stuck), or continue during the over power scram trip time. Indeed, contrary to power reactors, research reactor operation is characterized by frequent core modifications as a result of changes in experimental needs. Practically, each core modification must satisfy a number of safety criteria. Hence, it is desirable for the operator to have at his disposal means to perform simple and realistic transient estimations, even if only for scooping purposes. The objective of the present work is, precisely, to provide a simple and accurate model for predicting the dynamic response of MTR reactors under undesirable control rod withdrawal. This approach is based on coupled kinetics and thermal-hydraulic modeling. The core thermal hydraulic is computed on the basis of a one-dimensional description, through the conservation of mass, energy and momentum equations. The present model is used to simulate Egypt's second research reactor, ETRR-2, as an MTR-type. ETRR-2

Scientific paper
UDC: 621.039.572:532.54:536.24
BIBLID: 1451-3994, *21* (2006), 2, pp. 21-32

Authors' addresses:
[1] Mechanical Power Engineering Department, Cairo University, Giza, Egypt
[2] ETRR-2, Atomic Energy Authority 13759, Abuzabal, Egypt

E-mail address of corresponding author:
talal22969@yahoo.com (T. Abu-El-Maty)

is a light water, cooled, beryllium reflected, with an open chimney in an open pool type of a reactor. The nominal core power is 22 MW, plate-type fuel elements, with 19.7% enrichment. The fuel elements are boxes (8 8 cm), with 19-plane fuel plates each. The fuel active length is 80 cm, active width 6.4 cm. Core configuration is as shown in fig. 1.

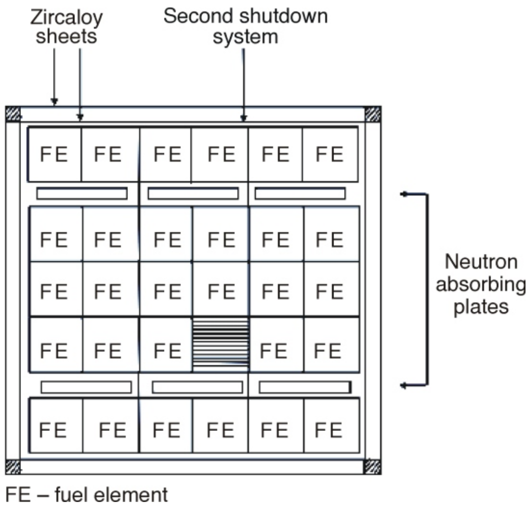

Figure 1. ETRR-2 core configuration

Coupled mechanisms and absorbing plates are used for reactor control and shutdown. A step-by-step motor produces the normal displacement of the control rod through a piston and cylinder set. For fast insertion, a pneumatic system is used. The fast shutdown is carried out by means of a compressed air injection from the tank to the cylinder piston set and the disconnection of the electromagnet that holds the piston.

MATHEMATICAL DYNAMIC MODEL

Numerical solution of point reactor kinetic equations

The average core power density $n(t)$ is calculated from a point reactor kinetics model with six groups of delayed neutrons. Generalized Runge-Kutta methods introduced by J. Sanchez [10] are used for the solution of stiff systems of ordinary differential equations. This method is representative of a class of stiff systems; in turn, this class is a member of a set of different approaches developed for the same purpose [11-13]:

$$\frac{\mathrm{d}n(t)}{\mathrm{d}t} \quad \frac{\rho(t) \quad \beta}{\Lambda} n(t) \quad \sum_{j \quad 1}^{6} \lambda_j c_j(t)$$
$$\frac{\mathrm{d}c_i(t)}{\mathrm{d}t} \quad \frac{\beta_i}{\Lambda} n(t) \quad \lambda_i c_i(t), \qquad i \quad 1,\ldots,6 \qquad (1)$$
$$\frac{\mathrm{d}\tau}{\mathrm{d}t} \quad 1$$

Reactivity feedback calculations

The reactivity feedback is calculated as the summation of feedbacks resulting from changes in the mean moderator density ($\delta\rho_c$), mean fuel temperature (δT_F), mean coolant temperature (δT_C) and the voidage caused by cladding thermal expansion changes (δY_{thex}) [14]. The hot channel contribution in feedback calculations is considered through the hot channel weighting factor ($1/N_{CHN}$) contribution, where N_{CHN} represents the total number of coolant channels:

$$\rho_{fb}(t) \quad \rho_{fb,v}(t) \quad \rho_{fb,f}(t) \quad \rho_{fb,c}(t) \quad \rho_{fb,thex}(t)$$
$$\rho_{fb}(t) \quad \alpha_v \ \delta\rho_c \quad \alpha_f \ \delta T_F \quad \alpha_C \ \delta T_C \qquad (2)$$
$$\alpha_v \ \delta Y_{thex}$$

Thermal-hydraulic modeling in transient state

Thermal-hydraulic treatments of the transient fluid flow through reactor coolant channels have been introduced by J. E. Meyer [15] through the momentum integral model. Obenchain [16] modified the momentum integral model to be more conservative in reactor accident analysis. This modified momentum integral model is described in the following conservation equations of mass, momentum and energy, respectively:

$$\frac{\partial \bar{\rho}}{\partial t} \quad \frac{\partial G}{\partial z} \qquad (3)$$

$$\frac{\partial G}{\partial t} \quad \frac{\partial}{\partial z} \frac{G^2}{\rho} \qquad \frac{\mathrm{d}p}{\mathrm{d}z} \quad \frac{f}{2\bar{\rho}D_e}|G|G \quad \bar{\rho}g \qquad (4)$$

$$\rho \quad \frac{\partial H}{\partial t} \quad G\frac{\partial H}{\partial z} \quad 2q/D \qquad (5)$$

where

$$H \quad H_1(1 \quad x) \quad H_g x,$$

$$\bar{\rho} \quad \rho_v R \quad \rho_L(1 \quad R),$$

$$\frac{1}{\rho} \quad \frac{1 \quad x^2}{1 \quad R}\frac{1}{\rho_1} \quad \frac{x^2}{R}\frac{1}{\rho_g},$$

and

$$\rho \quad [\rho_1 x \quad \rho_g(1 \quad x)]\frac{\mathrm{d}R}{\mathrm{d}x}$$

The combination of mass and energy equations, however, describes the local fluid heating rates and, therefore, also yields the rates of the local coolant flow

$$\frac{\mathrm{d}G}{\mathrm{d}z} \quad \frac{\mathrm{d}\bar{\rho}}{\mathrm{d}H} \; \frac{\mathrm{d}H}{\mathrm{d}t} \tag{6}$$

Substitution from eqs. (3) and (5) into eq. (6) brings to

$$\frac{\mathrm{d}G}{\mathrm{d}z} \; \frac{G}{\rho} \; \frac{\mathrm{d}\bar{\rho}}{\mathrm{d}H} \; \frac{\mathrm{d}H}{\mathrm{d}z} \quad \frac{2q}{\rho\ D} \; \frac{\mathrm{d}\bar{\rho}}{\mathrm{d}H} \tag{7}$$

The coolant channel is divided into N-axial zones with $N+1$ coolant axial nodes. An explicit difference approximation is applied to eq. (7) at each coolant node in the coolant channel; the coolant inlet mass flow rate should be specified as a function of time, allowing for the local mass velocity to be calculated. A channel averaged mass flow rate is calculated at each time step. Coolant enthalpy at each coolant node is calculated by applying the difference approximation [17] to eq. (5). In the case of using the explicit difference technique, approximate stability limitation on a time step must be utilized [15]; hence, the coolant temperature at each coolant node may be calculated.

Temperature distribution in fuel and clad

To calculate the temperature distribution in the fuel and in the clad, the following one-dimensional, partially differential heat diffusion equation is adopted

$$\frac{\partial}{\partial t}(\rho c_p T) \quad \frac{\partial}{\partial x} \; k\frac{\partial T}{\partial x} \quad f_s \dot{q}_f(z) \tag{8}$$

where $f_s = 1$ in the fuel meat zone and $f_s = 0$ in the clad zone.

Both the fuel meat half thickness and clad thickness are divided into N-axial zones with $N+1$ axial nodes and divided into M1 and M2 radial elements, respectively.

Localized heat generation is determined from the calculated core averaged power density. When calculating the maximum heat flux in each channel, the axial power peaking factor is considered for the average channel, while the total power peaking factor is considered for the hot channel. The axial heat flux distribution is considered to be cosine shaped, with an extrapolation length. Local volumetric heat generation at any node is calculated as the integration of heat generation in the mesh element that contains the node at its center, divided by the element volume. An adiabatic boundary condition is applied in calculating the fuel centerline temperature, while a convective boundary condition is applied at the clad coolant interface.

Heat transfer coefficient calculations

The convective boundary condition is determined by calculating the heat transfer coefficient at different heat transfer regimes.

Single phase forced convection regime

For the turbulent regime Re >10000, the well-known Dittus-Boelter equation is used

$$\mathrm{Nu} \quad 0.023\mathrm{Re}^{0.8}\,\mathrm{Pr}^{0.4} \tag{9}$$

For the transition regime 2100<Re<10000, the Nusselt number is calculated through the interpolation between laminar and turbulent correlations.

For the forced laminar heat transfer, the Sieder and Tate correlation is used

$$\mathrm{Nu} \quad 1.68 \; \frac{\mathrm{Re\,Pr}}{L/\,De}^{1/3} \; \frac{\mu_{\mathrm{co}}}{\mu_{\mathrm{c}}}^{0.14} \tag{10}$$

Subcooled boiling

The heat transfer coefficient is calculated from the Chen [18] correlation, extended from the saturated boiling region to cover the sub-cooled boiling region, as well

$$\varphi(z) \quad h_{\mathrm{NCB}}[T_{\mathrm{C}}(z) \;\; T_{Sat}] \\ h_{\mathrm{Sp}}[T_{\mathrm{C}}(z) \;\; T_{\mathrm{co}}(z)] \tag{11}$$

The onset of nucleate boiling represents the limit at which subcooled boiling is initiated

$$T_{\mathrm{ONB}} \quad T_{\mathrm{Sat}} \quad (\Delta T_{\mathrm{Sat}})_{\mathrm{ONB}} \tag{12}$$

Bergles and Rohsenow have introduced the following correlation for estimating the degree of saturation above which the corresponding heat flux causes the formation of nucleation on the wall.

$$(\Delta T_{\mathrm{Sat}})_{\mathrm{ONB}} \quad 0.556 \; \frac{\varphi_{\mathrm{ONB}}}{1082P^{1.156}}^{0.463P^{0.0234}} \tag{13}$$

Saturated nucleate boiling

The Chen [18] is used to calculate the saturated boiling heat transfer coefficient. The assumption of superposition, similar to that used in the 'partially boiling' region for sub-cooled conditions, is used

$$h_{\mathrm{Tp}} \quad h_{\mathrm{NCB}} \quad h_{\mathrm{Sp}} \tag{14}$$

where h_{Tp} is the local heat transfer coefficient, h_{NCB} is the contribution due to nucleate boiling and h_{Sp} is the contribution due to single-phase convection

$$h_{\mathrm{Sp}} \quad 0.023 \; \frac{G(1 \quad X)D_{\mathrm{e}}}{\mu_1}^{0.8} \; \frac{\mu_1 Cp_1}{k_1}^{0.4} \; \frac{k_1}{D_{\mathrm{e}}} \; F \tag{15}$$

$$h_{\mathrm{NCB}}$$

$$0.00122 \; \frac{k^{0.79} c_{\mathrm{P}}^{0.45} \rho_1^{0.49}}{\sigma^{0.5} \mu_1^{0.29} i_{fg}^{0.24} \rho_{\mathrm{g}}^{0.24}} \; \Delta T_{\mathrm{SAT}}^{0.24} \Delta \mathrm{P}_{\mathrm{SAT}}^{0.75} (S) \tag{16}$$

Film boiling

Sub-cooled film boiling

This occurs at a relatively high heat flux, if the wall heat flux exceeds the critical heat flux. Mirshak, *et al.* [19] have correlated a wide Varity of data for the water flow in tubes and rectangular channels

$$(Q/A)_{\mathrm{CHF}} \quad 151(1 \quad 0.1198V)$$
$$(1 \quad 0.00914\Delta T_{\mathrm{SUB}})(1 \quad 0.19P) \tag{17}$$

Noubuaki Ohnishi [20] has suggested the following relation between subcooled film boiling, $h_{\mathrm{F,SUB}}$, and saturated film boiling, $h_{\mathrm{F,Sat}}$, heat transfer coefficients as a function of coolant velocity

$$\frac{h_{\mathrm{F,SUB}}}{h_{\mathrm{F,Sat}}} \quad 1 \quad \mathrm{f}(V)\Delta T_{\mathrm{SUB}}$$

$$\mathrm{f}(V) = 0.025 + 0.01(\mathrm{V} - 1) \quad V > 1.0 \tag{18}$$

$$\mathrm{f}(V) = 0.025 \qquad V \quad 1.0$$

Saturated film boiling

Since, in the quality region, flow-boiling crisis is primarily of a hydrodynamic nature, the critical enthalpy rise appears to characterize flow behavior better than the critical heat flux. The Westinghouse APD correlation for critical enthalpy [21] is adopted as an engineering correlation, in order to predict the critical enthalpy rise of the water flow

$$H_{\mathrm{crit}} \quad H_{\mathrm{in}} \quad 1230.368(H_{\mathrm{Sat}} \quad H_{\mathrm{in}})$$

$$[1918.816 \quad 5349.43\mathrm{e}^{\;0.4318 D_{\mathrm{e}}}] H_{fg} \mathrm{e}^{\;2.03\,10^{\;9}} G -$$

$$953.593 H_{fg} \mathrm{e}^{\;0.0048 L/D_{\mathrm{e}}} \quad 2604.94 H_{fg} \frac{\rho_{\mathrm{v}}}{\rho_1}$$

$$1274.56 H_{fg} \tag{19}$$

If the clad temperature exceeds the minimum stable film boiling temperature (T_{MSF}), the mode of heat transfer is film boiling. The heat transfer coefficient is calculated from Dougall [22]

$$h_{\mathrm{F,Sat}} \quad 0.023 \; \frac{\rho_{\mathrm{v}} D_{\mathrm{e}}}{\mu_{\mathrm{v}}} \; \frac{Q_1 \quad Q_{\mathrm{v}}}{A}^{0.8} \; \frac{k_{\mathrm{v}}}{D_{\mathrm{e}}} \; (\mathrm{Pr}_{\mathrm{v}})^{0.4} \tag{20}$$

where Q_1 and Q_{v} represent the volumetric flow of liquid and vapor.

Transition boiling (partial film boiling)

The correlation obtained from McDoough [23] data indicates that the heat transfer in transition boiling can be correlated as follows

$$q_{\mathrm{DNB}} \quad q_{\mathrm{TB}} \quad C[T_{\mathrm{C}}(z) \quad T_{\mathrm{DNB}}(z)] \tag{21}$$

where T_{DNB} is the clad temperature at critical heat flux [24], T_{C} (z) is the surface clad temperature. Noubuaki Ohnishi [20] introduced the following correlation for estimating the minimum stable film boiling temperature in sub-cooled boiling during a reactivity insertion accident (RIA):

$$\Delta T_{\mathrm{MSF}} \quad T_{\mathrm{MSF}} \quad T_{\mathrm{Sat}} \quad 5.1\Delta T_{\mathrm{SUB}} \quad 350 \tag{22}$$

$$q_{\mathrm{MSF}} \quad h_{\mathrm{SUB}}(T_{\mathrm{MSF}} \quad T_{\mathrm{CO}}) \tag{23}$$

Parameter C represents the slope of the line that connected the critical heat flux and the minimum stable heat flux, and it is defined as.

$$C \quad \frac{q_{\mathrm{DNB}} \quad q_{\mathrm{MSF}}}{T_{\mathrm{MSF}} \quad T_{\mathrm{DNB}}}$$

Hence, the transition boiling heat transfer coefficient is calculated as follows.

$$h_{\mathrm{TB}} \quad \frac{q_{\mathrm{TB}}}{T_{\mathrm{C}}(z) \quad T_{\mathrm{CO}}(z)} \tag{24}$$

Void fraction calculation

Void fraction in sub-cooled boiling

The equation used in PARET and in J. L. Munoz-Cobo [25] for estimating the void fraction in sub-cooled boiling is a simplified form of Zuber's equation [26] and it is given by

$$\frac{\partial R}{\partial t} \quad SU_{\mathrm{L}} \frac{\partial R}{\partial z} \quad \lambda_s R \quad \frac{F_s q}{h_{fg} \rho_{\mathrm{v}} D} \tag{25}$$

where S is the flow distribution parameter, λ_s is the bubble collapse frequency, and F_S is the fraction of heat that produce vapor. The four point explicit difference is adopted for calculating the vapor volume fraction as shown in P. Lax and B. Wendroff [17].

Void fraction in saturated boiling

In the case of saturated boiling, the mass fraction of vapor is obtained directly from the enthalpy definition, $X=(H-H_f)/H_{fg}$. In this case, having calculated X, the vapor volume fraction is obtained by applying the Martinelli-Nelson correlation [18].

Pressure drop calculations

For pressure drop calculations, the core exit pressure is taken as the reference pressure point. From, momentum eq. (4), the pressure drop along the core is calculated as follows:

$$\frac{\partial p}{\partial z} \quad \frac{f}{2\bar{\rho}D_e}|G|G \quad \bar{\rho}g \quad \frac{\partial}{\partial z}\frac{G^2}{\rho} \quad \frac{\partial G}{\partial t} \tag{26}$$

$$\Delta P_{tot} \quad \Delta P_{int} \quad \Delta P_{tra} \tag{27}$$

where P_{tot} is the total pressure drop from core inlet to core exit, P_{int} is the internal pressure drop, and P_{tra} is the transient acceleration pressure drop.

Kuo-Fu Chen [27] has introduced the following expressions for calculating the elevation (P_{el}), friction (ΔP_{fric}), and acceleration (P_{acc}) pressure drop components that are used in calculating the internal pressure drop:

$$\Delta P_{el}(z) \quad g \,{}_{0}^{z}\, \bar{\rho}(z)dz$$

$$\Delta P_{fric}(z) \quad \frac{G^2 f}{2\rho_1 D_e} \,{}_{0}^{z}\, \varphi^2(z)dz$$

$$\Delta P_{acc}(z) \quad G^2 \,{}_{0}^{z}\, \frac{d}{dz} \quad \frac{1}{\rho_m} \quad dz$$

$$\Delta P_{int} \quad \Delta P_{el} \quad \Delta P_{fric} \quad \Delta P_{acc} \tag{28}$$

where

$$\rho(z)_m \quad \frac{1}{\dfrac{x(z)^2}{R(z)\rho_g} \quad \dfrac{[1 \quad x(z)]^2}{\rho_1[1 \quad R(z)]}}$$

$$\varphi^2(z) \quad \frac{1 \quad x(z)}{1 \quad R(z)}^{1.75}$$

While the transient acceleration pressure drop has the rate of change of the averaged mass flow rated

$$\Delta P_{tra} \quad {}_{0}^{L}\, \frac{\partial \bar{G}}{\partial t} dz \tag{29}$$

$$\bar{G} \quad \frac{1}{L_I \quad L_o \quad L} \quad L_I G(1) \quad L_o G(N \quad 1)$$

$$Dz \,{}_{i\;2}^{N\;1}\, \frac{G(i) \quad G(i \quad 1)}{2} \tag{30}$$

where L is the fuel active length, L_I stands for the inlet non-fueled length, and L_o is the outlet non-fueled length.

MODEL VALIDATION

The present model is used to recalculate the benchmark problem [28] to be validated. The comparison holds in the case of low enriched uranium which includes a slow reactivity insertion of \$0.09/s (1 \$ is the reactivity that will make a reactor prompt critical) and fast reactivity insertions of \$1.5/0.5 s and \$1.35/0.5 s. The initial conditions of the reactor are: 1 W initial power, 1000 m^3/h core flow and 38 C core inlet temperature. The reactor is allowed to scram in all simulated transients. The scram is described by a linear reactivity insertion of –\$10 in 0.5 s. The safety system trip point is 12 MW, with a time delay of 25 ms. The main parameters calculated during the validation are the power response, net reactivity, maximum fuel center-

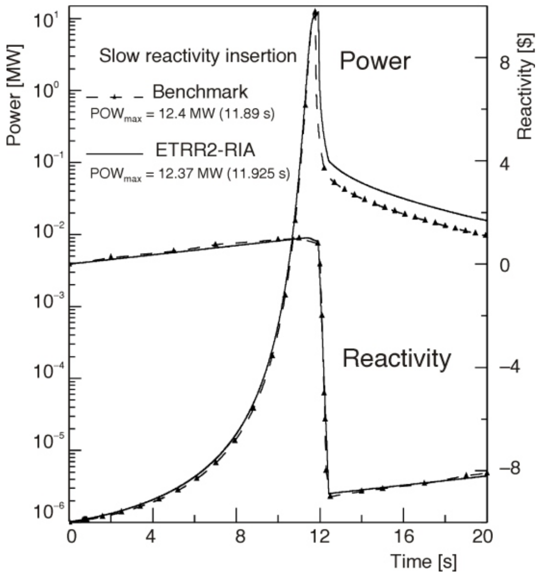

Figure 2. Power response for \$0.09/s with scram at 12 MW and a time delay of 25 ms

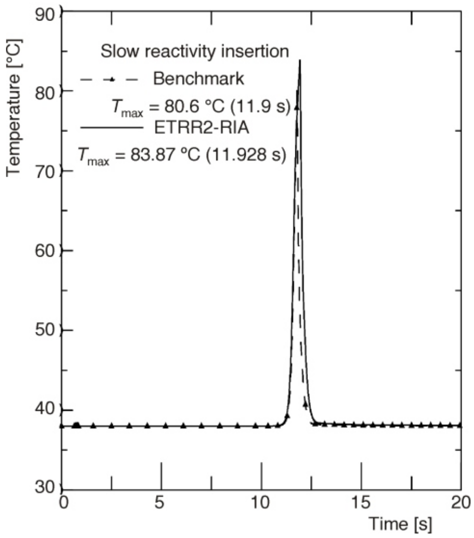

Figure 3. Fuel centerline temperature

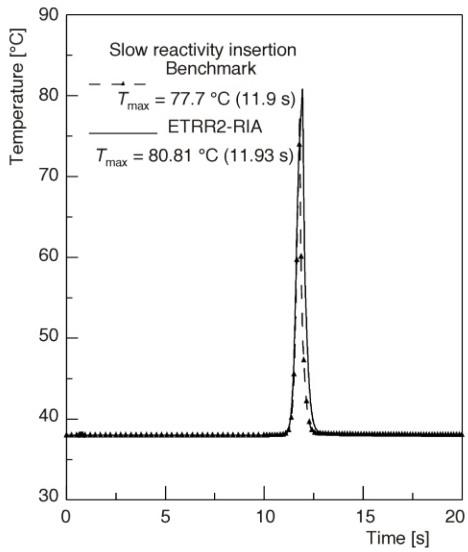

Figure 4. Clad temperature

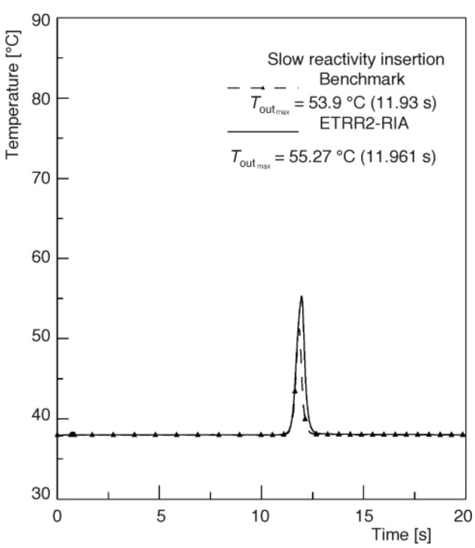

Figure 5. Coolant outlet temperature

line temperature, maximum clad temperature, and the coolant exit temperature. For the slow reactivity insertion transient of \$0.09/s, validation results are indicated in figs. 2 to 5, while for the fast reactivity insertion of \$1.5/0.5 s, they are given in figs. 6 to 9. Table 1 illustrates the peak values of power (P_m), fuel temperature ($T_{f,m}$), clad temperature ($T_{cl,m}$) and coolant outlet temperature($T_{co,m}$) with their times of occurrence for both benchmark data and ERTT2-RIA results. Also, this table illustrates the released energy at peak power time (E_{tm}). As shown in figures and illustrated in Table 1, a good agreement between the developed model results and benchmark results has been attained, hence the developed model has the capability to simulate RIA in MTR-type reactors.

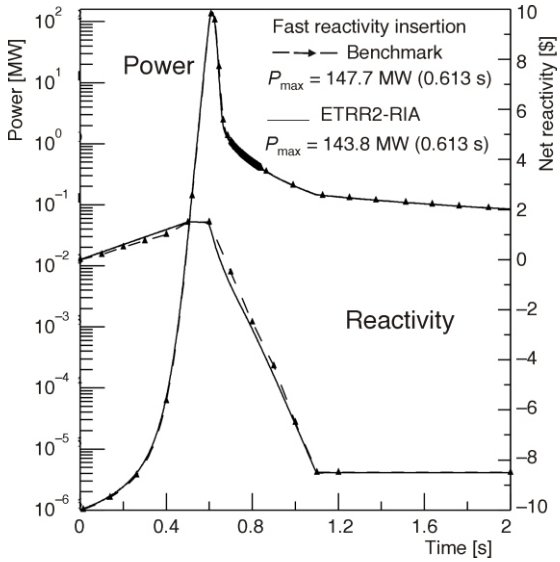

Figure 6. Power response for \$1.5/0.5 s insertion with scram at 12 MW and 25 ms delay

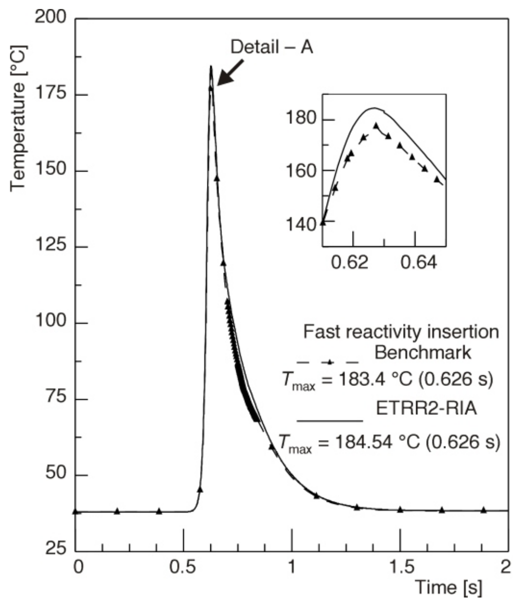

Figure 7. Fuel center line temperature

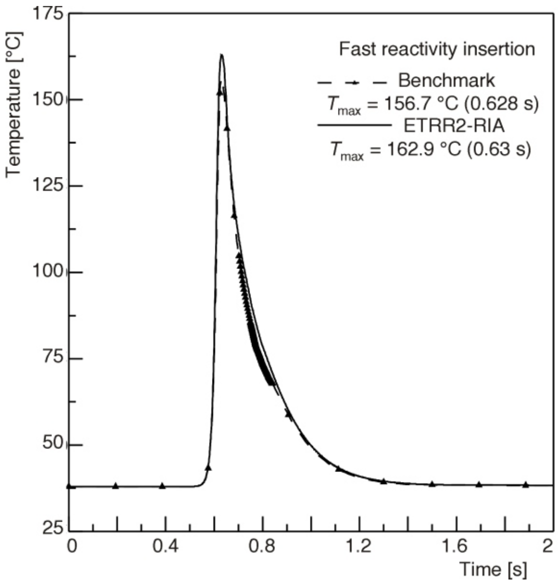

Figure 8. Clad temperature

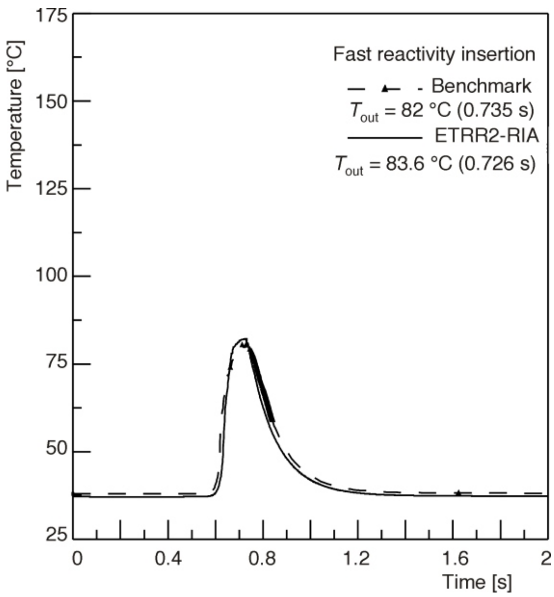

Figure 9. Coolant outlet temperature

Table 1. Comparison between ETRR2-RIA and the benchmark

Ramp [$/s]	$0.09/1.0 s		$1.35/0.5 s		$1.5/0.5 s	
	Benchmark	ETRR2-RIA	Benchmark	ETRR2-RIA	Benchmark	ETRR2-RIA
$P_m(t_m)$, [MW]	12.4 (11.89)	12.37 (11.925)	63.2 (0.693)	62.24 (0.693)	147.7 (0.613)	143.8 (0.613)
$T_{f,m}(t)$, [°C]	80.6 (11.9)	83.87 (11.93)	114.8 (0.714)	115.64 (0.713)	183.4 (0.626	184.54 (0.626)
$T_{cl,m}(t)$, [°C]	77.7 (11.9)	80.81 (11.93)	108 (0.717)	109.42 (0.717)	156.7 (0.628)	162.9 (0.63)
$T_{co,m}(t)$, [°C]	53.9 (11.93)	55.27 (11.96)	58.2 (0.862)	59 (0.831)	82 (0.735)	83.6 (0.726)
E_{tm}, [MJ]	4.549	4.63	1.54	1.565	2.95	2.98
At 20 s P [MW]	0.0146	0.0155				
E [MJ]	5.299	5.35				

RESULTS AND DISCUSSION

The ETRR2-RIA is used for simulating the uncontrolled withdrawal of a control rod, while assuming a linear relation between the withdrawal rod reactivity and its displacement. For a more conservative estimate, analysis is performed with a maximum withdrawal velocity of 16 cm/s and a control rod worth 3300 pcm (1 pcm = 10^{-5}). Taking these considerations into account, a $4/4 s insertion rate and $4 of total worth have been considered during simulations [29]. At the beginning of the transient, the critical core with 1W initial power, 1900 m^3/h coolant flow and 20 C core inlet temperature were considered. The scram system is available (transients with scram) when reactor power exceeds the over power safety setting (26.4 MW) with a 25 ms delay time before scram execution and a linear insertion of – $10 in 0.5 s, representing scram execution. The following simulated transients are based on different behaviors expected from the withdrawal rod at the moment of scram. The simulation is carried out according to different scenarios.

The withdrawal rod is reinserted into the core

Time behaviors of net reactivity, reactor power and released energy are shown in fig. 10. Net reactivity is increased linearly, from 0$ to a maximum value of 1.504 $, over 1.526 s. Just before the scram, negative feedback reactivity terminates the net reactivity increase at 1.481 $. A super prompt-critical transient is attained due to the high reactivity inserted (1.504 $), so, a rapid increase in reactor power, from 1W to a maximum value of

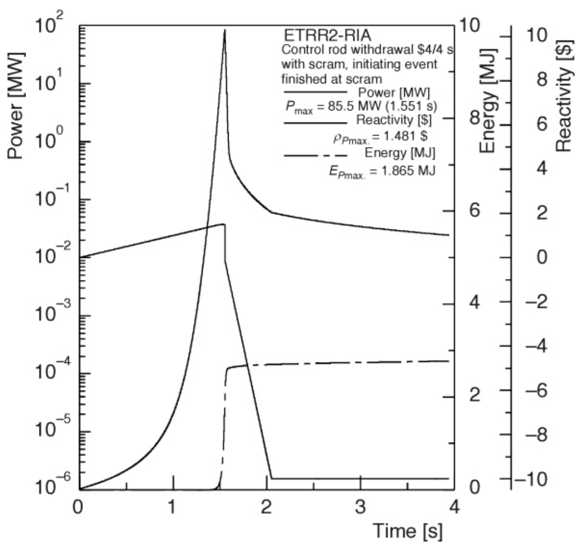

Figure 10. Power response for $4/4 s, with scram at 26.4 MW and a time delay of 25 ms

85.506 MW (1.551 s), is noticed. Due to a 25 ms delay time between the over power safety setting and scram execution, during the existence of the super-prompt critical condition, a high increase in power occurs, meaning that the actual triggering is executed at 85.506 MW, not at 26.4 MW. Thus, the scram system is ineffective during the fast transient. The withdrawal rod is reinserted into the core at a scram triggering time of (1.551 s), so that net reactivity slows down to – 0.0925 \$. Hence, it linearly decreases, due to both shutdown reactivity and the feedback mechanism. A fast decrease in the power of the response is followed by the decrease in net reactivity response. The released energy response is affected well by the power response, so a fast increase to 1.865 MJ is noticed at peak power time, while 2.771 MJ is attained at the end of the transient. The heat generated inside the fuel is also affected by the power response; so, a fast increase in fuel temperature, from 20 °C to a maximum value of 92.93 °C (1.557 s), is recorded. Thus, an increase in both the clad and coolant temperatures is produced. The maximum clad and coolant temperatures are 70.76 °C (1.569 s) and 31.53 °C (1.659 s), respectively, as shown in fig. 11. No boiling is predicted, since the maximum clad temperature is lesser than the boiling limit, and a complete shutdown margin is attained at the end of the transient.

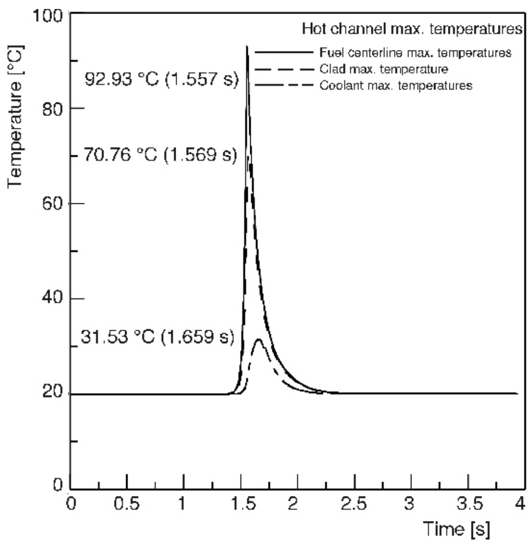

Figure 11. Temperature responses

The withdrawal rod is stuck in its position

The previous transient with all of its values and responses is repeated in the present transient up-to the time of scram triggering (1.551 s), when the ramp insertion (\$4/4 s) is changed to step insertion of 1.551 \$, due to the withdrawal rod being stuck. A competition between the positive reactivity inserted and, both the shutdown and feedback reactivity, results in a slow decrease in net reactivity after the scram. This slow decrease in net reactivity keeps the net reactivity in the super prompt-critical condition longer; as a result, the power increases to a maximum value of 130.55 MW over 1.571 s, as shown in fig. 12. All subsequent values increase as well, the released energy at peak power time to 4.156 MJ, peak fuel temperature to 193.18 °C(1.593 s), peak clad temperature to 144.73 °C(1.601 s) and peak coolant temperature to 58.23 °C(1.675 s), as shown in fig. 13. This transient indicates that the stuck in the withdrawal rod makes the scram system more ineffective to terminate the power, where the actual trip occurs

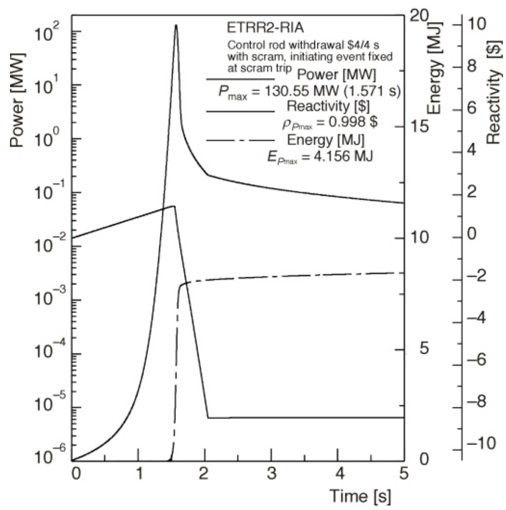

Figure 12. Power response for \$4/4 s, with scram at 26.4 MW and a delay of 25 ms

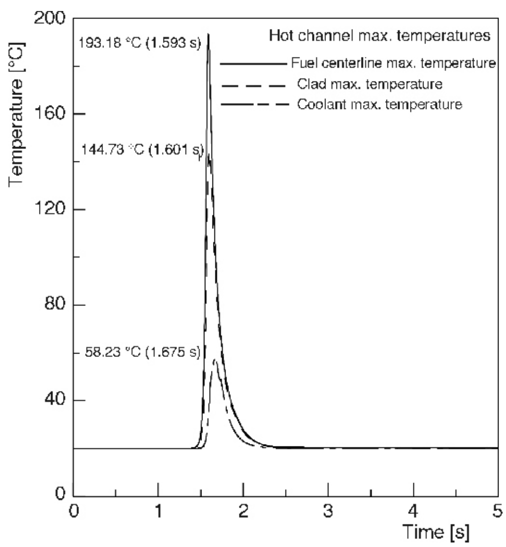

Figure 13. Temperature responses

at 130.55 MW. A partial boiling is predicted in the hot channel, since the maximum clad temperature exceeds the sub-cooled boiling limit. The shutdown margin is decreased to –8.449 \$ at the end of the transient and as a result of high temperatures attained, the maximum feedback reactivity is increased to –\$0.275.

The extraction of the withdrawal rod is continued after the scram

As mentioned before, the same transient is obtained up to the moment of the scram (1.551 s), but here the withdrawal of the rod continues, adding a ramp of \$4/4 s after the scram trip, so more positive reactivity is added during scram execution. As a result, the super prompt-critical condition is extended over a longer period of time and net reactivity decreases considerably after the scram, thus obtaining a higher rise in power. As shown in figs. 14 and 15, a peak power of 133.1 MW is attained at 1.571 s; hence, all subsequent values increase, the released energy at peak power time to 4.174 MJ, peak fuel temperature to 197 °C (1.593 s), peak clad temperature to 147.27 °C (1.601 s) and the peak coolant temperature to 60.3 °C (1.676 s). This transient has indicated that the continued withdrawal of the rod makes the scram system more and more ineffective to terminate the power where the actual trip occurs at 133.1 MW. A partial boiling is predicted in the hot channel since the maximum clad temperature exceeds the sub-cooled boiling limit and, also, the shutdown margin decreases to –6 \$ at the end of the transient. As a result, this transient is the worst of all presented, with reactor safety in the shutdown state reduced by 40%.

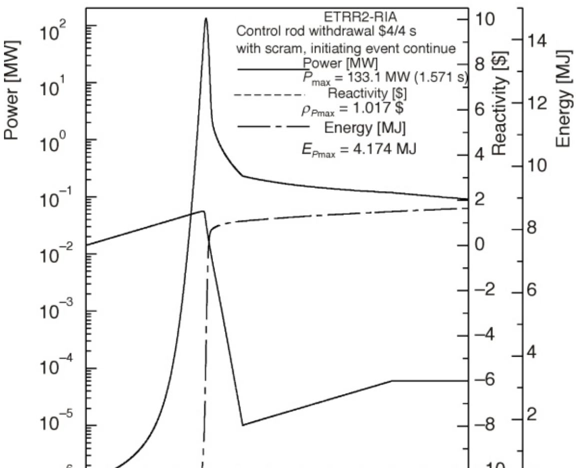

Figure 14. Power response for \$4/4 s, with scram at 26.4 Mw and a delay of 25 ms

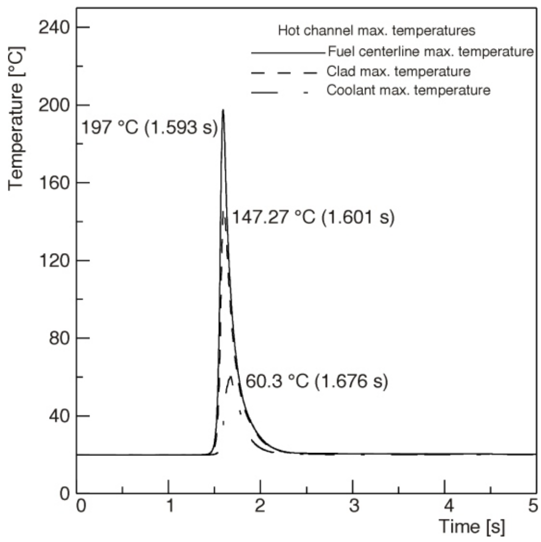

Figure 15. Temperature responses

Table 2 is a summary and comparison of relevant conclusions reached on the basis of results obtained during simulations of the uncontrolled withdrawal of control rods, according to different accident scenarios. The compared parameters are peak power with its time of occurrence $P_m(t_m)$, peak fuel temperature $T_{f,m}(t)$, peak clad peak temperature $T_{cl,m}(t)$, peak coolant temperature $T_{co,m}(t)$, the released energy at peak power time $E_{t,m}$, and the net negative reactivity after shutdown (ρ_c).

Table 2. Peak values for an uncontrolled withdrawal of the control rod (\$4/4 s)

Ramp (\$/s)	\$4/4 s – with scram		
	SEC4.1	SEC4.2	SEC4.3
$P_m(t_m)$, [MW]	85.5 (1.551)	130.55 (1.571)	133.1 (1.571)
$T_{f,m}(t)$, [°C]	92.93 (1.557)	193.81 (1.593)	197 (1.593)
$T_{cl,m}(t)$, [°C]	70.67 (1.569)	144.73 (1.601)	147.27 (1.601)
$T_{co,m}(t)$, [°C]	31.53 (1.659)	58.23 (1.675)	60.3 (1.676)
E_{tm} [MJ]	1.865	4.156	4.174
ρ_c [\$]	–10	–8.449	–6

CONCLUSION

A reactivity insertion accident can be simulated by the ETRR2-RIA program with a good degree of accuracy through various reactivity insertion scenarios. This program gives the reactor operator great flexibility in simulating different behaviors in accident scenarios or any other anticipated operational occurrences during the management of the reactor core. The compressed air which causes a forced scram in the ETRR-2 reactor is extremely important in accidents with a scram available scenario, because it may be overcome the initiating event. Hence, no boiling is predicted and a full shutdown margin is satisfied. Although the reactor shutdown system (scram) is ineffective in terminating the power rise in fast reactivity insertions (when the net reactivity inserted exceeds the delayed neutron fraction) for transients with scram, the ETRR2 core has withstood the uncontrolled withdrawal of the control rod in all simulated transients, since no clad melt down was predicted. The feedback mechanism plays an important role in terminating the net reactivity increase and in the shutdown of the reactor. The lower conductivity of the oxide fuel U_3O_8 has resulted in a much higher fuel temperature and low clad temperature, thus protecting the clad from melting.

APPENDIX

ETRR-2 main data

Axial peaking factor = 1.35
Total peaking factor = 3.0
Prompt neutron lifetime (l) = 75 μs
Effective delayed neutron fraction (β_{eff}) = 0.00705
Coolant temperature feedback coefficient
\$/°C = –1.3 10^{-2}
Void reactivity feedback coefficient
\$/%void = –0.2935
Fuel temperature feedback coefficient
\$/°C = –3.12 10^{-3}
Fuel thermal conductivity W/m K = 15
Clad thermal conductivity W/m K = 180

NOMENCLATURE

A – channel flow area, [m^2]
A_{PO} – outlet plenum
A_s – surface area, [m^2]
$C_i\,(t)$ – precursor concentration for delayed
C_p – specific heat, [J/kgK]
D – channel gap thickness, [m]
D_e – equivalent hydraulic diameter, [m]
f – friction factor for liquid flow
F_s – fraction of heat that produce vapor
g – acceleration of gravity, [m/s^2]
G_j – mass flux at node j, [kg/m^{2}s]
h – heat transfer coefficient, [W/m^2 °C]
H – enthalpy, [J/kg]
H_{fg} – latent heat of evaporation, [J/kg]
k – thermal conductivity
L – active fuel length, [m]
Nu – Nusselt number, ($= h\,D_e/k$)
P – pressure, [N/m^2]
Pr – Pradentel number, ($= \mu C_p/k$)
$\dot{q}_f$ – volumetric heat generation, [W/m^3]
q'' – surface heat flux, [W/m^2]
Re – Reynolds number, ($= GD_e/\mu$)
R_j – void fraction at node j
T – temperature, [°C]
$\bar{T}(j,t)$ – mean temperature at node j and time t
t – time, [s]
U, V – coolant velocity, [m/s]
W – channel width, [m]
W_h – active fuel width, [m]
x – radial distance, [m]
z – axial distance
X – steam quality
$X1$ – fuel half thickness, [m]
$X2$ – clad thickness, [m]

Greek symbols

α – thermal diffusivity, [m^2/s]
α_C – coolant feedback coefficient, [\$/°C]
α_f – fuel feedback coefficient, [\$/°C]
α_v – void feedback coefficient, [\$/%]
β – delayed neutron fraction for group
β_{eff} – effective delayed neutron fraction
β_i – delayed neutron fraction for group i
Λ – neutron generation time, [s]
λ_i – decay constant for a precursor group i
– specific volume, [m^3/kg]
μ – dynamic viscosity, [kg/m s]
σ – surface tension, [N/m]
ρ(t) – reactivity, [\$]
$\rho_{fb,c}$ – coolant feedback reactivity, [\$]
$\rho_{fb,f}$ – fuel feedback reactivity, [\$]
$\rho_{fb,thx}$ – reactivity feedback related to thermal expansion, [\$]
$\rho_{fb,v}$ – void feedback reactivity, [\$]
ρ_i – initiating event reactivity, [\$]
ρ_{sh} – shutdown reactivity, [\$]
ρ_λ – liquid density, [kg/m^3]
ρ_v – vapor density, [kg/m^3]
τ – time, [s]

Subscripts

av – average channel
cl – clad
co – coolant
f – fuel
ho – hot channel
I – inlet
l – liquid
NCB – nucleate boiling
o – outlet
ONB – onset of nucleate boiling
pl – plenum
Sat – saturated
Sp – single phase
Tp – two-phase
v – vapor

REFERENCE

[1] Woodruff, W. L., A Kinetic and Thermal-Hydraulic Capability for the Analysis of Research Reactors, *Nuclear Technology, 64* (1984), pp. 196-206
[2] Mirza, A. M., Khanan, S., Mirza, N. M., Simulation of Reactivity Transient Current MTRS, *Annals of Nuclear Energy, 25* (1998), pp. 1465-1484

[3] Nasir, R., Mirza, N. M., Mirza, S. M., Sensitivity of Reactivity Insertion Limits with Respect to Safety Parameters in a Typical MTR, *Annals of Nuclear Energy, 26* (1999), pp. 1517-1535

[4] Housiadas, C., Simulation of Loss of Flow Transients in Research Reactors, *Annals of Nuclear Energy, 27* (2000), pp. 1683-1693

[5] Khedr, A., D'Auria, F., Adorni, M., The Effect of Code User and Boundary Conditions on RELAP Calculations of MTR Research Reactors Transient Scenarios, *Nuclear Technology & Radiation Protection, 20* (2005), 1, pp. 16-22

[6] Khedr, A., D'Auria, F., Nodalization Effects on RELAP5 Results Related to MTR Research Reactor Transient Scenarios, *Nuclear Technology & Radiation Protection, 20* (2005), 2, pp. 3-9

[7] Bousbia-Salah, A., Jirapongmed, A., Hamidouche, T., White, J. R., D'Auria, F., Adorni, M., Assessment of RELAP5 Model for the University of Massachusetts Lowell Research Reactor, *Nuclear Technology & Radiation Protection, 21* (2006), 1, pp. 3-12

[8] Simth, R. S., Woodruff, W. L., NATCON, Steady state Thermal Hydraulics Code for Natural Convection in Research Reactors, RERTR Program, Argonne National Laboratory, 1987

[9] Woodruff, W. L., Hanan, N. A., Smith, R. S., Matos, J. E., A Comparison of the PARET/ANL and RELAP5/MOD3 Codes for the Analysis of IAEA Benchmark Transients, International Meeting on Reduced Enrichment for Research and Test Reactors, October 7-10, 1996, Seul, Republic of Korea

[10] Sanchez, J., On the Numerical Solution of the Point Reactor Kinetics Equations by Generalized Runge-Kutta Methods, *Nuclear Science and Engineering, 103* (1989), pp. 94-99

[11] Brown P. N., Hindmarsh, A. C., SIAM, *J. Numer. Analysis, 23* (1986), p. 610

[12] Watkins, D. S., Hansonsmith, R. W., ACM, *Trans. Math. Software, 9* (1983), p. 293

[13] Watts, H. A., Shampine, L. F., ACM, *Trans. Math. Software, 2* (1976), p. 200

[14] Housiadas, C., Lumped Parameter Analysis of Coupled Kinetics and Thermal-Hydraulic for Small Reactor, *Annals of Nuclear Energy, 29* (2002), pp. 1315-1325

[15] Meyer, J. E., Hydrodynamic Models for the Treatment of Rreactor Thermal Transients, *Nuclear Science and Engineering, 10* (1961), pp. 269-277

[16] Obenchin, C. F., PARET-A Program for the Analysis of Reactor Transients, ACE Research and Development Report, IDO-17282, 1969

[17] Lax, P., Wendroff, B., Systems of Conservation Laws, *Comm. On Pure and Appl. Math., 13* (1960), pp. 217-237

[18] Collier, J, G., Thome, J. R., Convective Boiling and Condensation, Oxford Science Publications, 3rd ed., 1996

[19] Rohsenow, W. M., Choi, H. Y., Heat, Mass, Momentum Transfer, Prentice-Hall Inc., Englewood Cliffs, NJ, USA, 1961

[20] Nobuaki, O., Kiyomi, I., Sadanitsu, T., A Study of Subcooled Film-Boiling under Reactivity-Initiated Accident Conditions in Light Water Reactors, *Nuclear Science and Engineering, 88* (1984), pp. 331-341

[21] Tong, L. S., Currin, H. B., DNB (Burnout) Studies in an Open Lattice Core, USAEC Report WCAP-3736, 1964

[22] Dougal, R. S., Rohsenow, W. M., Film Boiling on the Inside of Vertical Tubes with Upward Flow of the Fluid at Low Qualities, MIT Report 9079-26, 1963

[23] McDoough, J. B., Milich, E., King, E. C., An Experimental Study of Partial Film Boiling Region with Water at Elevated Pressure in a Round Vertical Tube, A.I.Ch.E. Preprint No. 29, Fourth National Heat Transfer Conference, 1960

[24] Bernath, L., A Theory of Local-Boiling Burnout and Its Application to Existing Data, *Chem. Eng. Prog.*, Symp. SER. 56, No. 30, 1960, pp. 95-116

[25] Munoz-Cobo, J. L., Chiva, S., Sekhri, A., A Reduced Order Model of BWR Dynamics with Subcooled Boiling and Modal Kinetics: Application to Out of Phase Oscillations, *Annals of Nuclear Energy, 31* (2004), pp. 1135-1162

[26] Zuber, N., Stube, F. W., Bijwaard, G., Vapor Void Fraction in Subcooled-Boiling and in Saturated Boiling Systems, *Proceedings*, Third International Heat Transfer Conference, Chicago, IL, August 7-12, 1966, American Institute of Chemical Engineering, New York, 1966, Vol. V, pp. 24-38

[27] ***, KUO-FU CHEN, Effect of System Pressure On Reactor Power Limits Criteria, Nuclear Reactor safety, July 14, 1992

[28] ***, IAEA (1980, 1992), Research Reactor Core Conversion from the Use of Highly Enriched Uranium to the Use of Low Enriched Uranium Fuels, Guidebook, Reports IAEA-TECDOC-233, IAEA-TECDOC -643

[29] ***, Atomic Energy Authority and INVAP (1999), final Safety Analysis Report. ETRR-2 Document, 0767-5325-3IBLI-001-1A, Egypt

Хани КАТЕР, Талал АБУ-ЕЛ-МАТИ, Салах ЕЛ-ДИН ЕЛ-МОРШДИ

ТЕРМОХИДРАУЛИЧКО МОДЕЛОВАЊЕ АКЦИДЕНАТА РЕАКТИВНОСТИ У МТР РЕАКТОРИМА

У раду је описан развој динамичког модела за термохидрауличку анализу МТР истраживачких реактора током акцидената насталих уношењем реактивности. Модел повезује реакторску кинетику са повратном реактивношћу и термохидраулику реакторског језгра. Ради представљања реакторског језгра разматране су две врсте канала: умерени и врући канали. Развијени рачунарски програм написан у ФОРТРАН-у компилиран је и коришћен на стоном рачунару. Модел је проверен на сигурносним прорачунима бенчмарка реактора МТР типа, који припадају генеричком IAEA 10 MW реактору, за прелазна стања настала спорим и брзим уношењем реактивности. Показало се добро слагање приказаног модела и бенчмарк прорачуна. Потом је модел коришћен за симулирање неконтролисаног извлачења контролне шипке ЕТРР-2 реактора у прелазном режиму при заустављању реактора услед прекорачења снаге. Анализирани су и критички испитани резултати овог модела за ЕТРР-2 реактор.

Кључне речи: акцидент унете реактивности, истраживачки реактор, термохидраулика, сигурносна анализа